2023, 20(3 Suppl.): 1078-1085
https://dx.doi.org/10.21123/bsj.2023.7937
P-ISSN: 2078-8665 - E-ISSN: 2411-7986
Baghdad Science Journal

Study the Chemical Bonding of Heterometallic Trinuclear Cluster Containing Cobalt and Ruthenium: [(Cp*Co) $(CpRu)_2$ (μ^3-H) (μ-H)$_3$] using QTAIM Approach

Ahlam Hussein Hassan * and Muhsen Abood Muhsen Al-Ibadi

Department of Chemistry, College of Science, University of Kufa, Najaf, Iraq.
*Corresponding Author.

Received 12/02/2023, Revised 09/10/2022, Accepted 11/10/2022, Published 20/06/2023

Abstract

The topological parameters of the metal-metal and metal-ligand bonding interactions in a trinuclear tetrahydrido cluster [(Cp*Co) (CpRu)2 (μ3-H) (μ-H)3]1 (Cp* = η5 -C5Me4Et), (Cp = η5 -C5Me5), was explored by using the Quantum Theory of Atoms-in-Molecules (QTAIM). The properties of bond critical points such as the bond delocalization indices δ (A, B), the electron density ρ(r), the local kinetic energy density G(r), the Laplacian of the electron density ∇2ρ(r), the local energy density H(r), the local potential energy density V(r) and ellipticity ε(r) are compared with data from earlier organometallic system studies. A comparison of the topological processes of different atom-atom interactions has become possible thanks to these results. In the core of the heterometallic tetrahydrido cluster, the Ru2CoH4 part, the calculations show no existence of any bond critical points (BCP) or identical bond paths (BPs) between Ru-Ru and Ru-Co. Electron densities are determined by the position of bridging hydride atoms coordinated to Ru-Ru and Ru-Co, which significantly affects the bonds between these transition metal atoms. On the other hand, the results confirm that the cluster under study contains a 7c–11e bonding interaction delocalized over M3H4, as shown by the non-negligible delocalization index calculations. The small values for electron density ρ(b) above zero, together with the small values, again above zero, for Laplacian ∇2ρ(b) and the small positive values for total energy density H(b), are shown by the Ru-H and Co-H bonds in this cluster is typical for open-shell interactions. Also, the topological data for the bond interactions between Co and Ru metal atoms with the C atoms of the cyclopentadienyl Cp ring ligands are similar. They show properties very identical to open-shell interactions in the QTAIM classification.

Keywords: AIM approach, Bonding analysis for the trinuclear cluster, DFT calculation, Topological properties, and trinuclear tetrahydrido cluster.

Introduction

Due to their possible uses in catalytic or stoichiometric reactivity, there has been much investigation into the activation of transition metal clusters in the inorganic and organometallic chemistry disciplines due to their potential benefits in catalytic or stoichiometric reactivity[1]. Cluster complexes differ from mononuclear complexes in their reactivity in that they can coordinate with substrate molecules many times and form a multi-electron transfer to the substrate [2,3]. Releasing bridging hydrido ligands from the polyhydrido cluster spontaneously produced multiple unoccupied coordination sites on the neighboring metal centers[4–6]. Because of the very high electron density at the transition metal atoms of the plolyhydrido clusters having cyclopentadienyl ligands, the reactivity was

2023, 20(3 Suppl.): 1078-1085
https://dx.doi.org/10.21123/bsj.2023.7937
P-ISSN: 2078-8665 - E-ISSN: 2411-7986
Baghdad Science Journal

increased toward splitting inactive chemical bonds, such as the C−C and C−H bonds of alkanes[7]. In modern quantum chemistry, Bader's theory of atoms in molecules (QTAIM)[8] is a good and complementary tool to the molecular orbital theory for interpreting the bonding and predicting the properties of the molecular structures[9,10]. The key concept in the QTAIM theory is the distribution function of the electron density ρ(r). The topological properties of ρ(r) and its derivatives play a significant role in the metal-metal and metal-ligand interaction in organometallic compounds through valence bonds and non-valence interactions [11–13]. Unfortunately, few publications have been published on the topology of the electron density in trinuclear heterometallic clusters. Therefore, to offer a rather satisfying interpretation of the bonding interactions in these important classes of clusters, more QTAIM studies are needed. This paper aims to study the bonding by analyzing the electron density distributions and comparing different topological indicators for M-M, M-H ,and M-C bonds in trinuclear heterometallic tetrahydrido cluster: [(Cp*Co) $(CpRu)_2$ (μ^3-H) (μ-H)$_3$]**1** (Cp* = η^5 -C_5Me_4Et), (Cp = η^5 -C_5Me_5)[14], as displayed in Fig. 1. This trinuclear heterometallic cluster, which has bridging hydride ligands, offers an excellent possibility to probe fascinating comparisons between the several topological properties (local and integral) of the electron density of M-M interactions and the influence of the bridging hydride atoms on the different interactions. This study presents an excellent chance to investigate the topological characteristics of various bonding interactions inside this cluster.

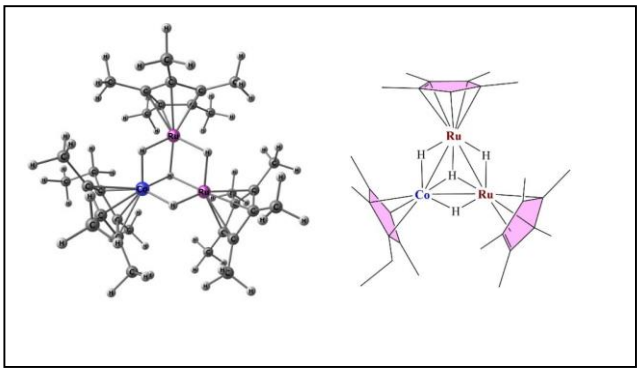

Figure 1. (I) the geometrical optimization structure of cluster 1 by chem craft, (II) by ChemDraw.

Materials and Methods

Computational Methods

The structure of X-ray diffraction for the heterometallic tetrahydrido cluster **1**, prepared by Suzuki and his co-workers[14], was used as starting point for geometrical optimization, which was carried out using the GAUSSIAN09[15] program. The PBE1PBE functional[16] has been used with the 6-31G (d,p) as a basis set for C and H atoms in addition to the LANL2DZ basis set, which is based on calculating Ru and Co metal atoms. QTAIM topological parameters have been performed with the AIM2000 program packages[17]. These calculations, applied to the theoretically optimized geometries, were carried out by using the PBE1PBE functional. The large all-electron "well-tempered basis set" WTBS [18,19] was used for the Ru and Co atoms, whereas the 6-31G (d, P) basis set was for other remaining atoms [20,21].

Results and Discussion

Electron Density Topological Analysis

Using the QTAIM method, we first investigate the presence of bonding interactions in the trinuclear heterometallic tetrahydrido cluster [(Cp*Co) (Cp $Ru)_2$ (μ_3-H) (μ-H)$_3$] **1** by using the QTAIM approach. Applying this method to cluster 1 gives the complete set of bond critical points (BCPs) together with the bond paths (BPs) that relate the bonded atoms and ring critical points (RCPs). Fig. 2 presents the molecular graph of the cluster.

2023, 20(3 Suppl.): 1078-1085
https://dx.doi.org/10.21123/bsj.2023.7937
P-ISSN: 2078-8665 - E-ISSN: 2411-7986
Baghdad Science Journal

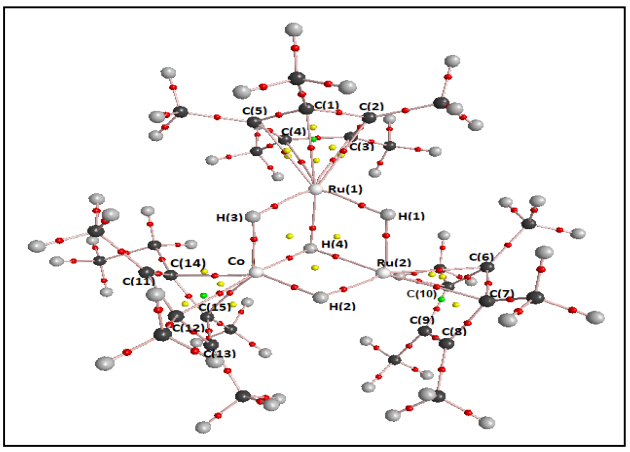

Figure 2. The Molecular graph of the Trinuclear heterometallic tetrahydrido cluster 1 is represented by a graph that highlights gray lines (bond paths BPs) with small red circles (bond critical points BCPs between two atoms), yellow circles (ring critical points RCPs) and green circles (cage critical points CCPs).

The BCPs and their BPs for the Co-H, Ru-H, C-H, Co-C, Ru-C, and C-C bonds were founded using the molecular graph. The Ru2CoH4 core hasn't BCPs and BPs between the hydride-bridge transition metal atoms, Co, Ru (1), and Ru (2). Then, we can assume that no direct M-M bonding exists[22]. Other ligands in bridging sits, such as carbonyl[23,24], Borylenes[25], and Alkynes[26], have also shown this loss of M-M bond paths. Also, RCPs located slightly closer to the geometrical centers of each M-H-M-H and Cp ligand were observed for cluster 1. A significant point of interest in this cluster is no direct bond-bond interaction between the transition metal atoms because there are no bond critical points, and bond paths are observed between the metal atoms. The absence of bond paths (BCPs) is hence no direct bonding interaction between these Ru-Ru and Ru-Co metallic atoms.

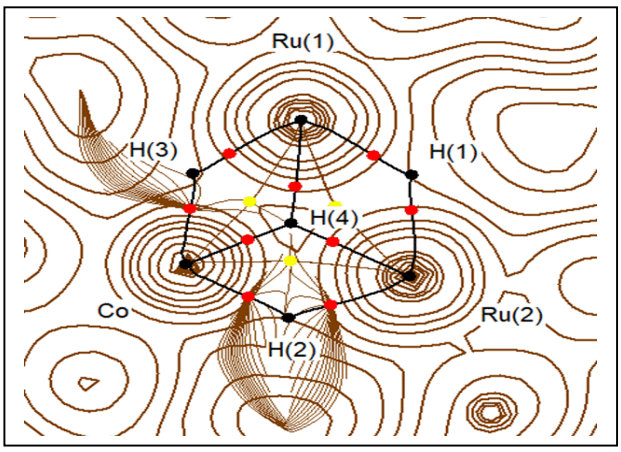

Figure 3. Gradient trajectories in the Co-H(3)-Ru(1)-H(1)-Ru(2)-H(2) plane mapped on an electron density plot, with atomic basins (BP's) and (BCP's), are indicated.

In Fig. 3, a gradient map for core plane Ru(1)-H(1)-Ru(2)-H(3) and (μ_3-H) with Ru(1), Ru(2), and Co, all BCPs and BPs with the atomic basins in the chosen planes are seen. In addition, the electron density distribution is very similar. It shows a significant charge density distribution around transition metal atoms Ru and Co, but no BCPs and BPs between Ru-Ru, and Ru-Co, were found. The BPs and BCPs located between Ru-H and Co-H are also shown.

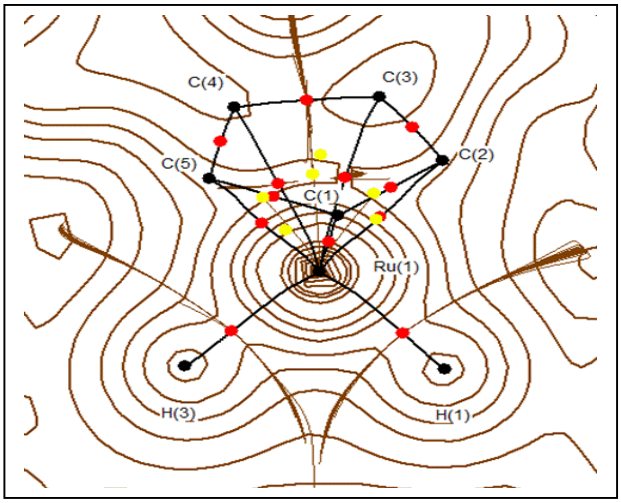

Figure 4. Gradient trajectories in the Cp ligand-Ru(1) plane with atomic basins (BCP's) and (BP's) are indicated.

Fig. 4, shows the BPs, BCPs, and RCPs associated with the tetrahydrido ligand attached to the ruthenium atom, Ru(1), and an electron density gradient map in this plane. The BCPs and BPs, found between Ru(1) with the five carbons CP atoms (C(1), C(2), C(3), C(4), and C(5)), located in and out this

2023, 20(3 Suppl.): 1078-1085
https://dx.doi.org/10.21123/bsj.2023.7937
P-ISSN: 2078-8665 - E-ISSN: 2411-7986
Baghdad Science Journal

plane, can also be observed. Additionally, H(1) and H(3) are shown on this plane.

Atoms in Molecules Analysis

The computed topological properties of the interactions between coordination bonds in the trinuclear heterometallic tetrahydrido cluster **1** are summarized in Table1.

Table 1. The topological parameters at BCPs [(ρ_b) electron density, ($\nabla^2\rho_b$) Laplacian, (H_b) ratio of total energy density, (G_b) ratio of kinetic energy density, (V_b) viral energy density, and (ε_b) ellipticity].

Bond	ρ_b(eÅ^{-3})	$\nabla 2\rho_b$(eÅ^{-5})	G_b(he^{-1})	H_b(he^{-1})	V_b(he^{-1})	ε_b
Ru1-H1	0.089	0.193	0.079	-0.031	-0.109	0.197
Ru1-H3	0.096	0.214	0.088	-0.035	-0.123	0.106
Ru1-H4	0.063	0.193	0.062	-0.014	-0.076	0.165
Ru2-H1	0.093	0.196	0.082	-0.033	-0.114	0.159
Ru2-H2	0.093	0.218	0.087	-0.032	-0.119	0.147
Ru2-H4	0.064	0.197	0.064	-0.015	-0.078	0.149
Co-H2	0.084	0.210	0.079	-0.026	-0.105	0.139
Co-H3	0.086	0.204	0.078	-0.027	-0.106	0.133
Co-H4	0.065	0.227	0.070	-0.014	-0.084	0.076
Ru1-C_{CP} [a]	0.077	0.250	0.080	-0.018	-0.098	0.992
Ru2-C_{CP}[a]	0.081	0.246	0.082	-0.021	-0.103	0.647
Co-C_{CP*} [a]	0.072	0.265	0.081	-0.014	-0.095	1.317
C_{CP}-C_{CP} [a]	0.284	-0.688	0.091	-0.263	-0.355	0.218

[a]Average values.

M-M interactions in clusters 1

Bader's quantum theory of atoms in molecules approach is a powerful tool to provide information about atoms and the nature of chemical bonding interaction[27,28]. Based on the QTAIM theory[29], the investigation of topological properties like $\nabla^2\rho_b$, the Laplacian of ρ, the electron density ρ_b, and the total energy density H_b at the BCPs are a helpful tool for the classification of chemical bonds[30,31].

The negative values of $\nabla^2\rho_b$ and H_b and large values of $\rho_b(r)$ are typical of Shared or open-shell (covalent) interactions. At the same time, small values of ρ_b, positive values of $\nabla^2\rho_b$, and H_b are typical of the Closed shell (ionic or van der Waals) interactions. The total energy density $H_b(r)$ is defined as $H_b(r) = G_b(r) + Vb(r)$, where $G_b(r)$ and $V_b(r)$ are the kinetic and potential energy density and has been identified as a more appropriate index than Laplacian to characterize an interaction[32]. The important point for M-M interactions is the total absence of any BCPs between any pair of the transition metal atoms bridged by hydride ligands. Thus, according to these results, we may say that there is no localized electron density between the M-M bond. According to the QTAIM model, defining and characterizing a chemical bond is associated with a found bond critical point [33]. The topological M…M bond was destroyed when the metal transition atoms were spanned by bridging hydride ligands (strong interaction). Depending on what is mentioned above, we conclude that there is no bond between transition metal atoms in this cluster. The absence of BCP between the metal-metal atoms has been observed, such as in bridged M…M interaction in the compounds $[Mn_3(\mu\text{-}H)_3(CO)_{12}]$, $[Tc_3(\mu\text{-}H)_3(CO)_{12}]$, $[Re_3(\mu\text{-}H)_3(CO)_{12}]$[34] and bridged Os…Os in clusters $[Os_3(l\text{-}H)(l\text{-}Cl)(CO)_{10}]$ and $[Os_3(l\text{-}H)(l\text{-}OH)(CO)_{10}]$[35]. However, BCPs and BPs between the metal-metal atoms have also been observed when there are strong ligand bridging interactions (μ^2-S), as in the case of Mo-Mo in the cluster $[Mo_3(\mu^2\text{-}S)_3(\mu^2\text{-}S)Cl_3(PH_3)_6]^+$ [36].

M-H interactions in cluster 1

For Co-H and Ru–H interactions, according to Table. 1, the electron density values at the BCPs are small, >1, within the range 0.063 to 0.096 eÅ^{-3}, though the Laplacian values are also small, again >1, 0.193 to 0.227 e Å^{-5}. These results added to the negative values for H_b, which are in the range of -0.014 to -0.035 he^{-1}, are in line with that of a typical open-shell bond (intermediate between ionic and covalent bonds) [31,37,38]. But the bonds of M-H4, the central hydride bridge, have noticeable topolectal properties. For instance, it is lower in the electron density and higher in the H_b values. In addition, the

2023, 20(3 Suppl.): 1078-1085
https://dx.doi.org/10.21123/bsj.2023.7937
P-ISSN: 2078-8665 - E-ISSN: 2411-7986
Baghdad Science Journal

values, slightly greater than zero, of the ellipticity for each of the Ru-H and Co-H bonds are typical of the straight bonding interactions between M and H atoms.

The Laplacian map computed to plane containing (Ru_2CoH_4) is very useful for the analysis of the M..M, and M-H interactions, displayed in Fig. 5. The pseudo-octahedral coordination of the Ru and Co atoms in this cluster is further evident in this figure, which also demonstrates how their valence shell charge depletion (VSCD) is almost perfectly cubic. Also, the VSCCs of hydrido bridge ligands are directed toward the midpoint between two atoms of transition metal to which they are bonded. The reasons for the absence of BPs and BCPs in the shape of the Laplacian distribution between Ru...Ru and Ru…Co suggests that there are no bonding electron pairs between these transition metal atoms.

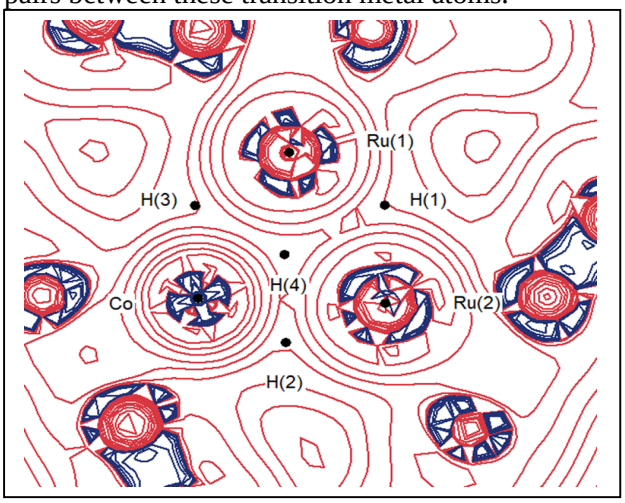

Figure 5. Laplacian map showing the electron density of Ru(1)-H(1)-Ru(2)-H(2)-Co-H(3) with H(4) plane in the trinuclear cluster 1.

M-Cp Interactions in cluster 1

The five BPs were given their BCPs between Ru and C atoms of the Cp ligand, which is a most notable aspect of the topological analysis for the Ru1-C interactions in this cluster, as shown in Fig. 2. Thus, it is fair to say that there is real chemical bonding between Ru metal and the carbon atom of Cp ligands and not just 'interactions' as has been previously found in other M-Cp interactions [39]. The calculated topological parameters for Ru-C and Co-C bonds are summarized in Table 1. As anticipated, the Ru-C, and Co-C bonds interactions, belong to the transit closed-shell category with positive values for ρ_b (between 0.077 and 0.081e Å^{-3}), the positive and small values of $\nabla^2\rho_b$ (between 0.246 and 0.265 e Å^{-5}) and negative, near-zero values of H_b (between -0.014 and -0.021 he^{-1}). These numbers align with those previously published in the literature[40]. Finally, the calculated ellipticities for the M-C bonds showed that the ellipticities average values of Co-Cp* interactions 1.317 are in most cases higher than the Ru-Cp bonds (ranging from 0.647-0.992). Large calculated values for the ellipticities indicated that the M-C bonds have a л character and are consistent with earlier research based on the MO theory [41].

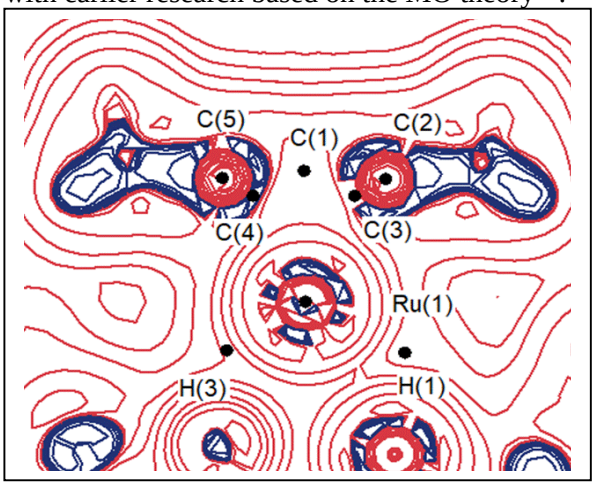

Figure 6. Laplacian map showing the electron density in the Ru-Cp plane.

Delocalization Indices.

The delocalization index, δ(A–B), is one of the best tools to estimate the number of delocalized electron pairs between two atoms [42,43]. Therefore, as listed in Table. 2, we calculated these indices as a tool to analyze a multicenter bonding in this cluster from one side and to describe different M…M interaction modes from another side[35].

Table 2. Delocalization indices of atom pairs interactions in cluster 1.

Atom pairs (A and B)	δ (A, B)	Atom pairs (A and B)	δ (A, B)
Ru1-H1	0.53	Ru1-C_{CP}	0.468
Ru1-H3	0.561	Ru2-C_{CP}	0.485
Ru1-H4	0.375	Co-C_{CP*}	0.409
Ru2-H1	0.551	Ru1...Ru2	0.417
Ru2-H2	0.556	Ru1...Co	0.342
Ru2-H4	0.384	Ru2...Co	0.349
Co-H2	0.468	Ru2...C_{CP}	0.407
Co-H3	0.463	Co…C_{CP*}	0.301
Co-H4	0.371		

2023, 20(3 Suppl.): 1078-1085
https://dx.doi.org/10.21123/bsj.2023.7937
P-ISSN: 2078-8665 - E-ISSN: 2411-7986
Baghdad Science Journal

The computed delocalization indices of M...M interaction values for this cluster (between 0.342 and 0.417) are higher than the reported hydride-bridged M...M nonbonding interaction values obtained in numerous other published QTAIM investigations. These studies showed that BCPs and BPs are not founded in several bridged M...M nonbonding interactions giving δ(A, B) values of 0.169-0.246, 0.177, and 0.208 for $[Ru_3(\mu\text{-}H)_2(\mu^3\text{MeImCH})(CO)_9]$[44], $[Os_3(\mu\text{-}H)(\mu\text{-}Cl)(CO)_{10}]$[35], and $[Fe_3(\mu\text{-}H)(\mu\text{-}COMe)(CO)_{10}]$[45], respectively. Alternatively, the calculated values of delocalization indices of the nonbonding M...M interaction of cluster **1** are comparable in magnitude to values found in many bridged M-M bond interactions (weak metal-metal interaction) such as Os-Os of the cluster $[Os_3(\mu\text{-}H)_2(CO)_{10}]$[35] (0.362). As a result, it is possible to say the value of δ(A–B) for each of the M…M bonds in cluster **1** is large enough to confirm that the M...M interaction is closer to the composition of its bond (weak metal-metal interaction) than its absence[35]. The values found for δ(M–H) in cluster **1** in the range 0.371-0.561 are similar to those obtained, for instance, for Os–H (in the field 0.426-0.449) and Ru–H (0.474) bonds of the clusters mentioned above [35,44]. Also, they are lower than that calculated for the complex terminal hydrido $[CrH(CO)_5]^-$ (0.59)[46] and close to $[Cr_2(\mu\text{-}H)(CO)_{10}]^-$ (0.38), especially the central hydride bridge δ (M-H4) values. It must be concluded that each of the four M-H bonds in cluster **1** has just half a shared electron pair. Because the sum of the δ(A–B) for the interactions in the core part $Ru_2Co(\mu\text{-}H)_3(\mu_3\text{-}H)$ of cluster **1** is 5.367. As a result, a multicenter 7c-11e interaction in this part of the molecule is suggested to explain the bonding in this cluster.

Conclusion

The Quantum Theory of Atoms-in-Molecules (QTAIM) approach is used to investigate the bonding in the trinuclear heterometallic tetrahydrido cluster $[(Cp^*Co)(CpRu)_2(\mu^3\text{-}H)(\mu\text{-}H)_3]$ **1**. The metal-ligand and metal-metal bond critical points (BCPs) properties the electron density (ρ_b), Laplacian ($\nabla^2\rho_b$), total energy density (H_b), kinetic energy density (G_b), viral energy density (V_b), and ellipticity (ε_b), as well as the delocalization indices δ(A, B), correspond with the computed data in the former organometallic systems studies. These results allowed a good comparison of the topological properties of various atom-atom interactions. A multicenter 7c–11e type is proposed in the bridged core part, $Ru_2Co(\mu\text{-}H)_3(\mu_3\text{-}H)$. Most intriguingly, the presence of bridging hydride ligands affects the electron density distribution of metal...metal interactions. No direct bonding has been observed due to the absence of BCPs and their BPs between these transition metals. The topological properties of the Ru-H and Co-H bonds indicate that they are all typical open-shell bonds.

Acknowledgment

The cooperation of the quantum group at Kufa University is appreciated.

Author's Declaration

- Conflicts of Interest: None.
- At this moment, We confirm that all the Figures and Tables in the manuscript are ours. Besides, the Figures and images, which are not ours, have been permitted republication and attached to the manuscript.
- Ethical Clearance: The project was approved by the local ethical committee at the University of Kufa.

Author's Contribution Statement

Manuscript preparation, computational analysis, and final editing: A.H.; manuscript review: M.A. All authors have read and agreed to the published version of the manuscript.

2023, 20(3 Suppl.): 1078-1085
https://dx.doi.org/10.21123/bsj.2023.7937
P-ISSN: 2078-8665 - E-ISSN: 2411-7986
Baghdad Science Journal

References

1. Cheng X, Lei A, Mei TS, Xu HC, Xu K, Zeng C. Recent Applications of Homogeneous Catalysis in Electrochemical Organic Synthesis. CCS Chem. 2022;4(4):1120-52. https://dx.doi.org/10.31635/ccschem.021.202101451
2. Muhsen Al-Ibadi MA, Taha A, Hasan Duraid AH, Alkanabi T. A theoretical investigation on chemical bonding of the bridged hydride triruthenium cluster: [Ru3 (μ-H)(μ3-κ2-hamphox-N,N)(CO)9]. Baghdad Sci J. 2020;17(2):488-93. https://dx.doi.org/10.21123/bsj.2020.17.2.0488
3. Chikamori H, Tahara A, Takao T. Transformation of a μ3-Benzyne Ligand into Phenol on a Cationic Triruthenium Cluster Supported by a μ3-Sulfido Ligand. Organometallics 2018;38(2):527-35. https://dx.doi.org/10.1021/acs.organomet.8b00832
4. Takao T, Suzuki H, Shimogawa R. Syntheses and properties of triruthenium polyhydrido complexes composed of 1,2,4-tri-tert-butylcyclopentadienyl and p-Cymene ruthenium units. Organometallics 2021;40(9):1303-13. https://dx.doi.org/10.1021/acs.organomet.1c00094
5. Daniels C, Gi E, Atterberry B, Blome-Fernández R, Rossini A, Vela J. Phosphine Ligand Binding and Catalytic Activity of Group 10–14 Heterobimetallic Complexes. Inorg Chem. 2022;61(18):6888-97. https://dx.doi.org/10.1021/acs.inorgchem.2c00229
6. AL-Nafee, M. Metal-Metal Bonding in Poly-Metallic Systems. PhD thesis, University of Oxford, 2019. https://ora.ox.ac.uk/objects/uuid:95f6c115-e1de-40b3-8f0b-eb6ce93e78b0
7. Kaneko T, Takao T. Reaction of a Triruthenium μ3-Borylene Complex with Benzonitrile: Formation of a μ3-η3-BCN Ring on a Cationic Ru3 Plane via Photo-Induced Intramolecular Borylene Transfer. Organometallics 2020;39(4):593-604. https://dx.doi.org/10.1021/acs.organomet.9b00831
8. Bader RFW. Atoms in Molecules A Quantum Theory. Oxford science publications. Clarendon Press; 1900. 438p. https://books.google.iq/books?id=up1pQgAACAAJ
9. Rampino S. Chemistry at the Frontier with Physics and Computer Science. Elsevier; 2022. Chap 14, The atom and the bond; p. 151-66. https://dx.doi.org/10.1016/b978-0-32-390865-8.00024-6
10. Wen L, Li G, Yang LM, Pan H, Ganz E. The structures, electronic properties, and chemical bonding of binary alloy boron–aluminum clusters series B4Aln0/−/+ (n = 1–5). Mater Today Commun. 2020;24(1):100914. https://dx.doi.org/10.1016/J.MTCOMM.2020.100914
11. van der Maelen JF, Ceroni M, Ruiz J. The X-ray constrained wavefunction of the [Mn(CO)4{(C6H5)2P-S-C(Br2)-P(C6H5)2}]Br complex: A theoretical and experimental study of dihalogen bonds and other noncovalent interactions. Acta. Crystallogr. B. Struct Sci Cryst Eng Mater. 2020;76(5): 802-814. https://dx.doi.org/10.1107/S2052520620009889
12. Malloum A, Conradie J. QTAIM analysis dataset for non-covalent interactions in furan clusters. Data Br. 2022;40(1):107766. https://dx.doi.org/10.1016/j.dib.2021.107766
13. Attia AS, Alfallous KA, El-Shahat MF. A novel quinoxalinedione-bicapped tri-ruthenium carbonyl cluster [Ru3(μ-H)2(CO)6(μ3-HDCQX)2]: synthesis, characterization, anticancer activity and theoretical investigation of Ru–Ru and Ru–Ligand bonding interactions. Polyhedron 2021;193(1):114889. https://dx.doi.org/10.1016/j.poly.2020.114889
14. Nagaoka M, Takao T, Suzuki H. Synthesis of a heterometallic trinuclear cluster containing ruthenium and cobalt and its reactivity with internal alkynes. Organometallics 2012;31(18):6547-54. https://dx.doi.org/10.1021/om300371g
15. Frisch MJ, Trucks GW, Schlegel HB, Scuseria GE, Robb MA, Cheeseman JR, et al. Gaussian 09, program, Revision A.02. Gaussian, Inc. Wallingford 2016. https://gaussian.com/g09citation/
16. Hirva P, Haukka M, Jakonen M, Moreno MA. DFT tests for group 8 transition metal carbonyl complexes. J Mol Model. 2008;14(3):171-81.
17. Biegler-König F, Schönbohm J. AIM2000. J Comput Chem. 2002;22(1):545-559. https://doi.org/10.1002/1096-987X(20010415)22:5<545::AID-JCC1027>3.0.CO;2-Y .
18. Al-Ibadi MAM, Alkurbasy NE, Alhimidi SRH. The topological classification of the bonding in[(Cp'Ru)2 (Cp'Os)(μ3-N)2(μ-H)3] cluster. AIP Conf Proc. 2019;2144(1):20009. https://dx.doi.org/10.1063/1.5123066
19. Alhimidi SRH, Al-Ibadi MAM, Hasan AH, Taha A. The QTAIM Approach to Chemical Bonding in Triruthenium Carbonyl Cluster:[Ru3 (μ-H)(μ3-κ2-Haminox-N, N)(CO) 9]. J Phys. 2018;1032(1):12068.
20. Al-Ibadi MAM, Oraibi DT, Hasan AH. The ruthenium-ruthenium bonding in bridged ligand system: QTAIM study of [Ru3(μ3-κ2-MeimCh) (μ-CO) (CO)9] complex. AIP Conf Proc. 2019;2144(1):20008. https://dx.doi.org/10.1063/1.5123065
21. Adamo C, Barone V. Toward reliable density functional methods without adjustable parameters: The PBE0 model. J Chem Phys. 1999;110(13):6158.
22. Yang X, Chin RM, Hall MB. Protonating metal-metal bonds: Changing the metal-metal interaction from bonding, to nonbonding, and to antibonding. Polyhedron 2022;212(1):115585. https://dx.doi.org/10.1016/j.poly.2021.115585

23. Cesari C, Bortoluzzi M, Forti F, Gubbels L, Femoni C, Iapalucci MC, et al. 2-D Molecular Alloy Ru–M (M = Cu, Ag, and Au) Carbonyl Clusters: Synthesis, Molecular Structure, Catalysis, and Computational Studies. Inorg Chem Published online September. 2022;61(37):14726–14741. https://dx.doi.org/10.1021/ACS.INORGCHEM.2C02099
24. Ruiz J, Sol D, Garciá L, Mateo MA, Vivanco M, Van Der Maelen JF. Generation and Tunable Cyclization of Formamidinate Ligands in Carbonyl Complexes of Mn(I): An Experimental and Theoretical Study. Organometallics. 2019;38(4):916–925. https://dx.doi.org/10.1021/acs.organomet.8b00898
25. Flierler U, Burzler M, Leusser D, Henn J, Ott H, Braunschweig H, et al. Electron-density investigation of Metal–Metal bonding in the dinuclear "Borylene" complex [Cp(CO)2Mn2(μ-BtBu)]. Angew Chem Int Ed Engl. 2008;47(23):4321–4325. https://dx.doi.org/10.1002/anie.200705257
26. Overgaard J, Clausen HF, Platts JA, Iversen BB. Experimental and theoretical charge density study of chemical bonding in a Co dimer complex. J Am Chem Soc. 2008;130(12):3834-43.
27. Domagała M, Lutyńska A, Palusiak M. Extremely Strong Halogen Bond. The Case of a Double-Charge-Assisted Halogen Bridge. J Phys Chem A. 2018;122(24):5484-92. https://dx.doi.org/10.1021/acs.jpca.8b03735
28. Prasad Kuntar S, Ghosh A, K. Ghanty T. Superstrong Chemical Bonding of Noble Gases with Oxidoboron (BO+) and Sulfidoboron (BS+). J Phys Chem A. 2022 126(43) 7888–7900. https://dx.doi.org/10.1021/acs.jpca.2c05554
29. Korabel'nikov D V, Zhuravlev YN. The nature of the chemical bond in oxyanionic crystals based on QTAIM topological analysis of electron densities. RSC Adv 2019;9(21):12020-12033. https://dx.doi.org/10.1039/c9ra01403a
30. Anil Kumar GN, Shruthi DL. The nature of the chemical bond in sodium tungstate based on ab initio, DFT and QTAIM topological analysis of electron density. Mater Today Proc Elsevier. 2021;44(8):3127-32. https://dx.doi.org/10.1016/j.matpr.2021.02.810
31. van der Maelen JF, Brugos J, García-Álvarez P, Cabeza JA. Two octahedral σ-borane metal (MnI and RuII) complexes containing a tripod κ3N,H,H-ligand: Synthesis, structural characterization, and theoretical topological study of the charge density. J Mol Struct. 2020;1201(127217):127217. https://dx.doi.org/10.1016/j.molstruc.2019.127217
32. F. Van der Maelen J. Topological Analysis of the Electron Density in the Carbonyl Complexes M(CO)8 (M = Ca, Sr, Ba). Organometallics 2019;39(1):132-41. https://dx.doi.org/10.1021/acs.organomet.9b00699
33. Gadre SR, Suresh CH, Mohan N, Kuznetsov ML. molecules Electrostatic Potential Topology for Probing Molecular Structure Bonding and Reactivity. Molecules 2021;26(11):3289. https://dx.doi.org/10.3390/molecules26113289
34. Van der Maelen JF, Cabeza JA. A topological analysis of the bonding in [M2(CO)10] and [M3(μ-H)3(CO)12] complexes (M = Mn, Tc, Re). Theor Chem Acc. 2016;135(3):1-11. https://dx.doi.org/10.1007/s00214-016-1821-0
35. Maelen JF van der, García-granda S, Cabeza JA. Theoretical topological analysis of the electron density in a series of triosmium carbonyl clusters: [Os3(CO)12], [Os3(μ-H)2(CO)10], [Os3(μ-H)(μ-OH)(CO)10] and [Os3(μ-H)(μ-Cl)(CO)10]. Comput Theor Chem. 2011;968(1-3):55-63. https://dx.doi.org/10.1016/j.comptc.2011.05.003
36. Feliz M, Llusar R, Andrés J, Berski S, Silvi B. Topological analysis of the bonds in incomplete cuboidal [Mo 3 S 4] clusters. New J Chem. 2002;26(7):844-50.
37. Nishide T, Hayashi S. Intrinsic Dynamic and Static Nature of π···π Interactions in Fused Benzene-Type Helicenes and Dimers, Elucidated with QTAIM Dual Functional Analysis. J Nanomater. 2022;12(3):321. https://dx.doi.org/10.3390/NANO12030321
38. Al-Kirbasee NE, Alhimidi SRH, Al-Ibadi MAM. QTAIM study of the bonding in triosmium trihydride cluster [Os3(μ-H)3(μ3-É2-CC7H3(2-CH3)NS)(CO)8]. Baghdad Sci J. 2021;18(4):1279-85. https://dx.doi.org/10.21123/BSJ.2021.18.4.1279
39. Van der Maelen JF, Gutiérrez-Puebla E, Monge A, García-Granda S, Resa I, Carmona E, et al. Experimental and theoretical characterization of the Zn—Zn bond in [Zn2 (η5-C5Me5) 2]. Acta Crystallogr B. 2007;63(6):862-8.
40. Helal SR, Al-Ibadi MAM, Hasan AH, Taha A. The QTAIM Approach to Chemical Bonding in Triruthenium Carbonyl Cluster: [Ru3 (μ-H)(μ 3-κ 2-Haminox-N,N)(CO)9]. J Phys Conf Ser. 2018;1032(1):12068. https://dx.doi.org/10.1088/1742-6596/1032/1/012068
41. Isaac C, Wilson C, Burnage A, Miloserdov M, Mahon M, Macgregor S, et al. Experimental and Computational Studies of Ruthenium Complexes Bearing Z-Acceptor Aluminum-Based Phosphine Pincer Ligands Inorg Chem. 2022;61(50):20690–20698. https://dx.doi.org/10.1021/acs.inorgchem.2c03665
42 Mercero JM, Ugalde JM. Atomic Clusters with Unusual Structure, Bonding and Reactivity. 1st Ed. Chap 2, Elsevier. Electron delocalization in clusters; 2022. p. 19-39. https://dx.doi.org/10.1016/B978-0-12-822943-9.00013-9
43. Bartashevich E v., Mukhitdinova SE, Tsirelson VG. Bond orders and electron delocalization indices for S–N, S–C and S–S bonds in 1,2,3-dithiazole systems. Mendeleev Commun. 2021;31(5):680-3. https://dx.doi.org/10.1016/j.mencom.2021.09.029

2023, 20(3 Suppl.): 1078-1085
https://dx.doi.org/10.21123/bsj.2023.7937
P-ISSN: 2078-8665 - E-ISSN: 2411-7986
Baghdad Science Journal

44. Cabeza JA, Van Der Maelen JF, Garcia-Granda S. Topological analysis of the electron density in the N-heterocyclic carbene triruthenium cluster [Ru3(μ-H)2(μ3- MeImCH)(CO)9] (Me2im = l,3-dimethylimidazol-2-ylidene). Organometallics 2009;28(13):3666-72. https://dx.doi.org/10.1021/om9000617
45. Al-Ibadi MAM, Kzar KO. Theoretical study of Fe-Fe bonding in a series of iron carbonyl clusters [(μ-H)2Fe3(CO)9(μ3-As)Mn(CO)5], [Et4N] [(μ-H)2Fe3(CO)9(μ3-As)Fe(CO)4] and [Et4N][HAs{Fe2(CO)6(μ-CO) (μ-H)}{Fe(CO)4}] by QTAIM perspective. Egypt J Chem. 2020;63(8):2911-20. https://dx.doi.org/10.21608/ejchem.2020.21235.2267
46. Macchi P, Donghi D, Sironi A. The electron density of bridging hydrides observed via experimental and theoretical investigations on [Cr2(μ2-H)(Co) 10]-. J Am Chem Soc. 2005;127(47):16494-504. https://dx.doi.org/10.1021/ja055308a

دراسة التأصر الكيميائي للعنقود ثلاثي النوى المحتوي على الكوبالت و الروثينيوم: [(Cp*Co) (Cp)$_2$ Ru)$_2$ (μ^3-H) (μ-H)$_3$] باستخدام نهج QTAIM

احلام حسين حسن و محسن عبود محسن

قسم الكيمياء، كلية العلوم، جامعة الكوفة، النجف الاشرف، العراق.

الخلاصة

المعلمات الطوبولوجية لتأثرات بين معدن-معدن ومعدن-ليكاند في العنقودي ثلاثي النوى رباعي الهيدريد[(Cp*Co) (CpRu)$_2$ (μ^3-H)$_3$]**1** (Cp* = η^5 -C_5Me_4Et), (Cp = η^5 -C_5Me_5)، باستخدام نظرية الكم للذرات في الجزيئات (QTAIM). خصائص النقاط الحرجة لاواصر مثل مؤشرات إلغاء تحديد الموقع δ (A, B) ، كثافة الإلكترون ρ(r)، كثافة الطاقة الحركية المحلية G(r)، (Laplacian) لكثافة الإلكترون $\nabla^2\rho(r)$، كثافة الطاقة المحلية H(r)، وكثافة الطاقة الكامنة المحلية V(r) والإهليلجيه ε(r) تمت مقارنتها بالبيانات مع دراسات للانظمة العضوية المعدنية السابقة. أصبحت مقارنة العمليات الطوبولوجية لتفاعلات الذرة والذرة المختلفة ممكنة بفضل هذه النتائج. في قلب مجموعة رباعي هيدرات المعادن غير المتجانسة ، الجزء Ru_2CoH_4 ، تُظهر الحسابات عدم وجود أي نقاط حرجة للتأصر (BCP)أو مسارات الاواصر (BPs) بين Ru-Ru و Ru-Co يتم تحديد توزيع كثافات الإلكترون من خلال موضع تجسير ذرات هيدريد المنسقة مع Ru-Ru و Ru-Co ، وهذا له تأثير كبير على تكوين الاواصر بين ذرات المعدن الانتقالي. من ناحية أخرى ، تؤكد النتائج أن المركب قيد الدراسة يحتوي على تفاعل تأصر 7c–11e غير محدد على M3H4 ، كما هو موضح في حسابات مؤشر إلغاء تحديد الموقع غير المهملة. تظهر القيم الصغيرة لكثافة الإلكترون ρ(b) فوق الصفر ، جنبًا إلى جنب مع القيم الصغيرة ، مرة أخرى فوق الصفر ، لـ Laplacian $\nabla^2\rho(b)$ والقيم الإيجابية الصغيرة لكثافة الطاقة الإجمالية H(b)، في تأصر Co-H و Ru-H تعتبر اواصر H في هذه المجموعة نموذجية لتفاعلات الغلاف المفتوح. أيضًا ، تتشابه البيانات الطوبولوجية لتفاعلات الاواصر بين ذرات المعدن Co و Ru مع ذرات C حلقة cyclopentadienyl Cp. تظهر خصائص مشابهة جدًا لتفاعلات الغلاف المفتوح في تصنيف QTAIM.

الكلمات المفتاحية: نهج AIM ، تحليل الترابط للكتلة ثلاثية النوى ، وحساب DFT ، والخصائص الطوبولوجية ، والكتلة ثلاثية النوى الرباعية الهيدريدو.